Membrane organization and regulation of cellular Cholesterol homeostasis

María S. Jaureguiberry[ξ], **M. Alejandra Tricerri**[ξ], **Susana A Sanchez**[δ], **Horacio A Garda**[ξ], **Gabriela S. Finarelli**[ξ], **Marina C. Gonzalez**[ξ], and **Omar J. Rimoldi**[ξ,*]

[ξ]Instituto de Investigaciones Bioquímicas de La Plata (INIBIOLP), CONICET/UNLP, Facultad de Ciencias Médicas, Calles 60 y 120, La Plata 1900, Buenos Aires, Argentina

[δ]Laboratory for Fluorescence Dynamics, University of California-Irvine, Irvine, CA

Abstract

An excess of intracellular free Cholesterol (Chol) is cytotoxic, and its homeostasis is crucial for cell viability. Apolipoprotein A–I (apoA-I) is a highly efficient Chol acceptor as it activates complex cellular pathways that tend to mobilize and export Chol from cellular depots. Here we hypothesize that membrane composition and/or organization is strongly involved in Chol homeostasis. To test this hypothesis, we constructed a cell line over expressing Stearoyl CoA desaturase (SCD-cells), which modifies plasma membrane (PM) composition by the enrichment of monounsaturated fatty,acids and determined this effect on membrane properties, cell viability and cholesterol homeostasis. PM in SCD-cells has a higher phospholipids/sphingomyelin ratio and is slightly enriched in Chol. These cells showed an increase in the cholesteryl esters/free Chol ratio, they were more resistant to Chol toxicity and in addition, they exported more caveolin than Control cells. The data suggest that cell functionality is preserved by regulating membrane fluidity and Chol exportation and storage.

Keywords

stearoyl CoA desaturase; human apolipoproteinA-I; membrane heterogeneity; cholesterol transport; Chinese Hamster Ovary Cells; Intracellular cholesterol storage; caveolin; cytotoxicity

Introduction

Chol plays several structural and metabolic roles which are crucial to human biology. Particularly, in membranes, it regulates fluidity and different cell signaling events by partitioning into domains of selective composition as caveolae and other sphingolipidrich domains (Jacobson et al., 2007). Cellular Chol can be synthesized *de novo* or incorporated via the uptake of Chol- containing lipoprotein particles. On the other hand, extra hepatic cells lack metabolic pathways for Chol catabolism, and thus the excess must be, either exported or recruited into non-toxic cellular compartments.

Although both mechanisms seem to be opposite, both depend on the cellular type, and on the intracellular trafficking which is regulated by several signaling pathways (Prinz, 2007). Chol is transported from the endoplasmic reticulum to the plasma membrane by protein-mediated and vesicular pathways. The signaling events involved are complex and not completely

understood. Sterol Carrier Protein 2 (SCP-2) has been related with different lipid transports, such as phosphatidylinositol, sphingomyelin and phospholipids. It has been involved in intracellular traffic of Chol to the PM and recent data show that SCP-2 interacts with caveolin-1, both within cytoplasm and at the PM (Schroeder et al., 2007) (Schroeder et al., 2001). Thus, a close interaction between these proteins seems to modify intracellular distribution of signaling lipids to PM lipid rafts/caveolae.

The apolipoprotein-mediated cellular Chol release requires a specific interaction of apolipoproteins with proteins on the cell surface. There is a large body of evidence that the ATP Binding Casette A1 (ABCA1) catalyzes the concurrent loading of apolipoproteins with phospholipids and Chol (Smith et al., 2004),but there are also different pieces of evidence indicating that these events occur separately in time and in different specialized domains of the cell membrane (Fielding et al., 2000) (Yancey et al., 2003). It was proposed that ABCA1 promotes flipping of lipids from the inner to the outer membrane leaflet by a process driven by its ATPase activity (Oram, 2002). Interestingly, there is some controversy on the role of lipid-rafts in Chol efflux. While Mendez et alsuggest that apoA-I preferentially acquires Chol from loosely packed microdomains (Mendez et al., 2001), Storey et al (Storey et al., 2007) demonstrated that apoA-I removes Chol with higher efficiency from lipid-raft. The molecular mechanisms of intracellular Chol pool mobilization toward the cell membrane mediated by apoA-I are also poorly understood. ABCA1 appears to favor the removal of Chol meant to be substrate for the esterifying enzyme acyl CoA: Chol acyltransferase (ACAT) (Oram and Heinecke, 2005) that would otherwise accumulate as cytosolic cholesteryl ester in lipid droplets. It was proposed that apoA-I induces the transport of intracellular Chol to cell-surface caveolae, possibly in part through the stimulation of caveolin expression (Sviridov et al., 2001).

There is strong evidence that lipid arrangement in biological membranes is heterogeneous. Small changes in physicochemical variables such as Chol content, variations of lipid head group chemistry, or protein interactions might induce growth or coalescence of certain types of lipid domains, which could in turn modulate membrane associated physiological signaling. In order to characterize the importance of membrane composition and lateral organization on Chol homeostasis, we constructed a stable cell line with a permanent modification in the PM lipids, and further analyzed the influence of this composition on the Chol homeostasis and cell viability. The overexpression ofstearoyl CoA desaturase (SCD-cells), alters the phospholipid fatty acid composition without changing the expression levels of ABCA1 (Sun et al., 2003).

Experimental procedures

Materials

ApoA-I from healthy human serum (kindly donated by Banco de Sangre, Instituto de Hemoterapia de la Provincia de Buenos Aires, La Plata, Argentina) was isolated and purified as previously described (Tricerri et al., 1998). Purity was higher than 95% as estimated by SDS polyacrylamide gel electrophoresis (SDS–PAGE) using Coomasie blue staining. Laurdan, (6-lauroyl-2-(dimethylamino) naphtalene) was purchased from Molecular Probes (Eugene, OR). Tris (hydroxymethyl) aminomethane hydrochloride (Trizma HCl), 3-[4,5-dimethylthiazol-2-yl]-2,5-diphenyl tetrazolium bromide (MTT), methyl β cyclodextrine (MβCD), Oil Red O and lipids used as standards for TLC (egg phosphatidylcholine, free and esterified cholesterol, brain sphingomyelin, phosphatidylinositol, phosphatidylserine and phosphatidylethanol amine) were obtained from Sigma-Aldrich Biochemicals (St. Louis, MO); Minimal essential medium (MEM) and the antibiotic-antimicotic mixture were obtained from Invitrogen Corporation (Carlsbad, CA, USA). Fetal bovine serum (FBS) was purchased from Bioser (Bs. As., Argentina) and [3H] Chol was obtained from Amersham Biosciences (Pittsburgh, PA, USA). Polyclonal anti-apoA-I antibody was obtained by injecting purified human apoA-I in rabbits

and further purification of the IgG fraction from plasma by Hi-trap columns (Pharmacia, Piscataway, NJ). A polyclonal anti-rat SCD-1 antibody was obtained by cloning the fragment corresponding to the 85 N-terminal amino acid section of the Cdna into the plasmid pGEX-4T-1 (Amersham Biosciences). The pGEX-SCD1 construct was expressed in *Escherichia coli* BL21 cells, and the GST fusion protein was purified according to the manufacturer's instructions. The purified bacterial expressed fusion protein was used as an immunogen on rabbit. Antibodies against ABCA1 and caveolin-1 proteins were purchased from Santa Cruz Biotech (CA, USA).

Methods

Construction of stable cell lines over expressing stearoyl CoA desaturase (SCD-cells) We created a stable cell line over expressing the enzyme Stearoyl-CoA-desaturase (SCD-1) according to (Sun et al., 2003). The full length SCD-1 cDNA was subcloned in the plasmid pcDNA3.1-Hygro, to generate pcDNA3.1-SCD-1, and the stable transfection was performed with lipofectAMINE 2000 (Invitrogen, Carlsbad, CA, USA). A clon resistant to hygromicin was selected, expanded and frozen in liquid N2 for further experiments. Cells transfected with the plasmid without the SCD-1 insert, were considered as control cells for all experiments.

The SCD1-mRNA overexpression in the selected clon was assessed by Northern blot analysis. Total cell RNA was isolated with a Wizard RNA isolation system (Promega, Madison, WI, USA) according to manufacturer´s instructions. Twenty micrograms of total RNA were size fractionated on a 1% agarose/formaldehyde gel and then transferred to a Zeta-Probe nylon membrane (Bio-Rad, Richmond, CA, USA). SCD-1, and β-actin probes were prepared by incorporating [32P] deoxycytidine 5'-triphosphate by random prime labeling. Northern blot hybridization analyses were performed as described by Sambrook et al. (Sambrook et al., 1989). The radioactive signals for mRNAs of SCD-1 were quantified using a Phosphorimager apparatus (Molecular Dynamics, Sunnyvale, CA, USA). Signal was normalized to mRNA for β-actin with the desaturase mRNA probed on the same gel. Next we verified the protein level in our stable cell line by western blot analysis.

Total cell protein samples (150 μg per lane) were analyzed by sodium dodecyl sulfate polyacrylamide gel electrophoresis and blotted onto Hybond-ECL nitrocellulose membrane (Amersham Biosciences, Little Chalfont, UK). The membrane was probed with the anti-SCD-1 antiboby (1:1,000 dilution) and then with horseradish peroxidase conjugated anti-rabbit (Sigma-Aldrich, St Louis, MI) (1:3,000 dilution), using PBS (phosphate saline buffer pH 7.5), containing 3% nonfat dried milk, for saturation and incubation with antibodies. Washes were carried out with PBS as well. Peroxidase activity was revealed using Pierce ECL Western blotting substrate (Pierce, Rockford, IL, USA).

In addition, we analyzed membrane fatty acid composition. Briefly, cellular fractions corresponding to plasma membrane were isolated (see below), lipids extracted according to Folch et al. (Folch et al., 1957),and samples esterified with F3B at 64°C for 3h. Fatty acid composition of cell total lipids was determined by gas–liquid chromatography (GLC) of their methyl esters. Samples were injected into an Omega Wax 250 (Supelco, Bellefonte, PA, USA) capillary column of 30 m, 0.25-mm inner diameter and 0.25 μm film. The temperature was programmed to obtain a linear increase of 3°C/min from 175 to 230°C. The chromatogram peaks were identified by comparison of their retention times with those of authentic standards (Grain Fatty Acid Methyl Ester Mix (Supelco, Bellefonte, PA, USA).

Finally, we checked by western blot the ABCA1 protein expression in our cell line compared to control cells, in order to discard alterations in its level due to the desaturase overexpression.

Cell culture

Cells were cultured as described by Gonzalez et al (Gonzalez et al., 2008). Chinese hamster ovary (CHO-K1) cells were seeded in 10 cm diameter plates andincubated until confluence in minimal essential medium (MEM) supplemented with penicillin/streptomycin solution (100 units/mL) and 10% FBS at 37°C in a 5% CO_2 atmosphere.

Evaluation of cellular free and esterified Chol

Control and SCD-cells were grown until confluence. Following, cell monolayers were washed with PBS and incubated overnight with serum-free medium containing 0.5µCi/mL [3H] Chol, and 2 mg/mL BSA. After 24 h equilibration with MEM containing 1mg/mL of BSA, monolayers were washed twice with PBS and treated for 12 h with serum free medium, containing or not 12 µg/mL of apoA-I. Media were collected, and cells scrapped for lipid extraction by the method of Bligh and Dyer (Bligh and Dyer, 1959). Sterol species were separated by high performance thin layer chromatography (HPTLC) on a silica gel plate with concentrating zone (Whatman, Schleier-Schuell, England) and developed in hexane/ethyl ether/acetic acid (80:20:1, by vol). Lipid spots corresponding to cholesteryl esters (CE) and unesterified Chol (FC) were identified by staining with I2 vapor and co-migration with authentic standards. Appropriate spots were scrapped and quantified by scintillation counting.

Membrane isolation and lipid characterization

We followed the technique of Mander et al (Mander et al., 1994),with further modifications. Cell monolayers were grown to confluence, washed three times with PBS, scrapped and resuspended in 900µl buffer 10mM HEPES, 0.25M Sacarose, 1mM EDTA pH 7.4, in order to get about $1.5-2 \times 10^7$ cells/mL. Cells were lysed in a glass to glass homogeneizer with ~ 20 strokes, and centrifuged at $16.000 \times g$ for15 min. A gradient of Nicodenz-Ficoll was hand-made by the step-by step addition of 45% Nicodenz solution followed by Ficoll gradient between 1 and 22%. The supernant of the cell sample was loaded on top of the test tube and ultracentrifuged in a L8.70M Ultracentrifuge at $238.000 \times g$, in a SW 60 Ti Rotor (Beckman Coulter, Fullerton, CA) for 16 h at 4oC. Two hundred µL fractions were collected from the top of the gradient tube, protein content in each fraction was measured (Bradford, 1976), and fractions corresponding to plasma membrane pooled and characterized using standard enzyme markers and electron microscopy. Lipids were extracted according to the procedure of Blight and Dyer (Bligh and Dyer, 1959) and separated by thin-layer chromatography (TLC) on silica gel G 60 plates with concentrating zone (Merck, Darmstadt, Germany). We used two successive development systems for polar lipids chloroform/methanol/ammonium/water (70:25:3.5:1.5, by vol) and chloroform/methanol/acetic acid/water (80:10:2:0.76, by vol), followed by a mixture to better develop neutral lipids petroleum ether/ethyl ether/acetic acid (80:20:1, by vol). Then, the plate was spread with ethanol- sulfuric acid 5% and heated until complete calcination. Spots corresponding to each lipid were identified with appropriate standards and quantified by using the Image Quant software (Amersham Biosciences, Piscataway, CA, USA).

Cell viability

Control and SCD-cells (with or without the addition of 20 µg/mL apoA-I) were incubated as described above, and the 3-[4,5-dimethylthiazol-2-yl]-2,5-diphenyl tetrazolium bromide (MTT) reduction assay was carried out as previously described (De Felice et al., 2001). Briefly, cells were incubated with 0.5 mg/mL MTT at 37°C for 4 h to allow MTT reduction to formazan blue by metabolically active cells. One hundred µl of 0.01 N HCl containing 10% SDS was added and kept overnight to each well, to lyse cells and to solubilize formazan crystals. Optical density was measured at 570 nm in a DTX 880 Multimode Detector (Beckman Coulter, Fullerton, CA). In a separate experiment, media were collected and the release of the

cytoplasmic enzyme Lactate dehydrogenase (LDH) was measured by decrease of Optical density at 340 nm (commercial kit, Wiener lab, Rosario, AR).

Oil Red O Lipid droplets Staining

Intracellular neutral lipids were stained with Oil-Red. Briefly, cell monolayers were rinsed with PBS, and fixed for 1 h with PBS + 10% formaldehyde. Next, staining was performed by covering with 0.5 % Oil-Red in isopropanol for 2 h, followed by extensive washing. Representative photomicrographs are shown for Control and SCDcells.

Laurdan Generalized Polarization (GP) imaging and quantification

Laurdan is used as a membrane probe because of its large excited-state dipole moment, which results in its ability to report the extent of water penetration into the bilayer surface as a result of the dipolar relaxation effect (Weber and Farris, 1979)..Water penetration has been correlated with lipid packing and membrane fluidity (Parasassi et al., 1997). If Laurdan is solubilized in a lipid structure (i.e a membrane), its spectrum will sense the environment and shift according to the water content of the bilayer. The quantification of the spectral shift is given by

$$GP = I440 - I490/I\,440 + I490 \tag{1}$$

where $I440$ and $I490$ are the emission intensities at 440 and 490 nm, respectively. A full discussion of the use and mathematical significance of GP can be found in the literature (Bagatolli et al., 2003) (Parasassi and Gratton, 1995) (Sanchez et al., 2007a; Sanchez et al., 2007b). Images were collected on a scanning two photon fluorescence microscope designed at the Laboratory for Fluorescence Dynamics (University of California at Irvine, CA) as described previously (Sanchez et al., 2007a; So et al., 1995).. A mode-locked titanium sapphire laser (Mira 900; Coherent, Palo Alto, CA) pumped by a frequency doubled Nd:vanadate laser (Verdi; Coherent) set to 780 nm was used as the two-photon excitation light source. The microscope set up was fixed as described before. A two channel detection system was attached for GP image collection (Sanchez et al., 2007a).. The fluorescence was split in two channels using a Chroma Technology 470DCXR-BS dichroic beam splitter in the emission path. Interference filters (Ealing 490 and Ealing 440) were placed in the emission paths to further isolate the two desired regions of the emission spectrum (440 +/− 10 nm and 490 +/−10 nm), which were collected simultaneously by separate detectors. Two simultaneous 256×256 pixel images (centered at 490 nm emission, and centered at 440 nm emission) were obtained from the cells, which were processed applying the GP formula (equation 1) to each pixel using the SimFCS program (Laboratory for Fluorescence Dynamics). Corrections for the wavelength dependence of the emission detection system were accomplished through the comparison of the GP value of a known solution (Laurdan in DMSO) (Sanchez et al., 2002) taken on an ISS Inc. model PC1 steady-state fluorometer and then in the microscope. SCD or control cells were grown as described previously until ~70% confluence (in order to allow the observation of single cell membranes) and Chol removal induced by incubation overnight with 20 µg/mL apoA-I in serum-free medium, or by 10 mM MβCD for 30 min. Following, cells were washed with PBS, and incubated for 15 min at 37°C with Laurdan to a final concentration 1 µM in DMEM + 2.5% FBS, next cells were washed and kept in DMEM, at the same temperature during the observation time in a thermostatized microscope stage.

Other analytical methods

Protein was quantified by the method of Lowry et al. (Lowry et al., 1951).

Transmission electron micrograph was acquired at the Centro de microscopía electrónica, Facultad de Veterinaria, UNLP, AR. Western blotting for the detection of apoA-I and

caveolin-1, was performed by traditional techniques as described above. In order to better determine the significance of intracellular levels of caveolin, 4 lines of each, Control and SCD-cells were loaded into a gel and probed with a-caveolin, following stripping and re probing against a-β actin as a housekeeping marker. Chol efflux toward MβCD or apoAI was measured with the Amplex Red Commercial kit (Invitrogen, Carlsbad, CA, USA).

Unless otherwise stated, results were means ± S.E. of three independent measurements. Statistically significant differences between experimental conditions were evaluated by ANOVA followed by Bonferroni's comparison test (* $P < 0.05$ compared to control).

Results

Cell line construction

SCD catalyzes the conversion of stearoyl-CoA to oleoyl-CoA, and thereby it regulates the ratio of monounsaturated to saturated fatty acids in cell membrane phospholipids (Enoch et al., 1976). The efficiency of SCD transfection and overexpression was confirmed by different methods. Northern blot showed high levels of ARNm as compared with almost undetectable amounts in the control cells (Figure 1a); the same was observed when analyzing, by western blotting, protein expression levels (Figure 1b). In this case, an upper faint band was observed with the same intensity for both types of cells, fact that was assumed as the endogenous Hamster SCD. Moreover, as expected (Sun et al., 2003) ABCA1 protein basal level was not significantly modified in SCD-cells with respect to control (Figure 1c)

Plasma membrane isolation and composition

Plasma membrane was isolated and lipid composition characterized. Figure 1d shows a typical elution profile of the cell fractionation obtained by ultracentrifugation. Selected fractions were pooled and further characterized. As the electron microscopy image shows (Figure 1e), sample rearranged as close empty vesicles (as typically occurs with membrane preparations), and it was free of mitochondria. Plasma membrane was confirmed by the presence of the standard enzyme marker Na-K ATPase, and showed no contamination with endoplasmic reticulum (undetectable arylesterase activity). Figure 2 shows the comparative lipid composition of the isolated plasma membrane in SCDversus control cells. As expected, a significant increase in the 16:1/16:0 and 18:1/18:0 ratios confirmed the enzyme activity (Figure 2a). In good agreement with Sun et al (Sun et al., 2003), there was ~ a 100% increase in SCD-cells of both ratios as compared with Control cells. Following, we analyzed the relative composition of the major neutrallipids. In an attempt to facilitate the comparative studies, we expressed the lipids as the mass ratio of glycerophospholipids (GPL) to sphingomyelin (SM), and glycerophospholipids to free Chol (FC). Figure 2b shows that SCD cells have over 50 % higher GPL/SM ratio, instead the GPL/FC ratio decreased by about 20%. The values in Control cells were in good agreement with previous data by Cezanne et al (Cezanne et al., 1992).

Membrane organization of cells *in vivo*

Our group (Sanchez et al., 2002) (Sanchez et al., 2007a) (Tricerri et al., 2005) and others (Gaus et al., 2003) (Heiner et al., 2008) (Montes et al., 2007) (Smith et al., 2001) have previously used Laurdan GP imagining and two-photon excitation fluorescence microscopy in order to analyze membrane organization in artificial bilayers and in live cells. This technique offers the sole advantage of allowing the analysis of lateral organization without disruption of the observation system. Laurdan solubilizes equally into fluid or condensed membranes and is not associated with specific fatty acids or phospholipid head groups (Bagatolli et al., 2003). Thus GP values reflect the overall membrane structure and not a specific lipid or protein composition (Harris et al., 2002).

Laurdan-labeled cells were imaged by setting the focal z plane in the middle of the cell, allowing the observation of PM (Figure 3a). GP values can range from 1 to −1 according to equation (1), and an arbitrary color scale was used to visualize pixels with different GP values. Using the SimFCS program one can separate pixels associated with the plasma membrane (Figure 3b), and select areas in which GP can be quantified without "contamination" of cellular debris present in the image (Figure 3b, white empty circles). GP value was the average of the pixel distribution in the selected area (histogram in Figure 3c). In order to avoid dispersion in the results due to laser alignment, cell confluence, etc, each treatment with Chol acceptors (apoA-I or ciclodextrine) was compared to untreated cells measured in the same day under exact conditions.

This study shows two interesting issues

i) Even though some heterogeneities in the GP images could suggest presence of domains in the plasma membrane (Figure 3a and b), we cannot clearly confirm the presence of "macro domains" in the cells, as it is easily defined with artificial liposomes (Tricerri et al., 2005). As Laurdan GP imaging can distinguish liquid-ordered (lo) and liquid disordered (ld) macro domains coexisting in the same bilayer (Sanchez et al., 2007a) (So et al., 1995), we attributed this observation to the fact that domains are dynamic and move within the experimental time, and thus they are not usually detectable in live cells. Instead, Sun et al (Sun et al., 2003) using the same SCD construct and triton X-100 visualized in the PM of fixed cells, domain segregation with an increased amount of ld. It is possible that the fixing and detergent treatment "freeze" the mobile existing membrane segregations.

ii) In spite of the different lipid composition (Figure 2), no significant changes in the membrane overall water content (i.e fluidity) were observed between SCD-cells and the Control (Figure 3d and e). Instead, when Chol was removed, GP changes depended on the cell type and the Chol acceptor. When apoA-I is used as Chol acceptor, the GP value decreased in both cases (Figure 3d). Instead, if MβCD was used as acceptor, membrane GP increased for the Control cells and decreased for SCD-cells (Figure 3e). To compare the efficiency of both acceptors, we measured Chol in the media at the end of the incubation times. ApoA-I-mediated Chol efflux was about half efficient than MβCD, which was also faster under the experimental conditions. In this case, higher amounts of Chol were solubilized from SCD-cells (Figure 4).

Effect of SCD overexpression on cell functionality

We investigated the influence of SCD overexpression on mitochondrial reduction capacity. This test is widely used and has been inversely correlated with cytotoxicity (Melchert et al., 2001). Thus, higher OD at 560 nm was related with an increased activity of metabolic cells, which induced the cleavage of the yellow tetrazolium salt MTT to purple formazan crystals. SCD-cells showed ~ 17% higher mitochondrial activity (Figure 5a) than control cells. Moreover, the incubation with apoA-I induced a higher MTT reduction activity in both type of cells. In addition, we measured the release of LDH,which was correlated with cytotoxicity (Peter et al., 2008). Control cells showed a higher release of LDH to the medium, indicating that SCD overexpression induces a beneficial effect on cell viability (Figure 5b).

Intracellular Chol esterification and lipid storage

Since intracellular Chol could be freed or stored as Cholesteryl esters, we measured radioactivity incorporated in CE after incubating cells with [3H] Chol as described above, in the presence or absence of apoA-I. Our results showed a higher CE/FC ratio in SCD-cells in comparison with Control cells (not shown). It is well-known that in skin fibroblasts (Yamauchi et al., 2004) and in CHO cells (Gonzalez et al., 2008), apoA-I induced a decrease in the cellular Chol pool available to be esterified by ACAT. Thus, a decrease in CE/FC ratio was expected

when control cells were incubated with apoA-I, and the same was observed when apoA-I was incubated with SCD cells (not shown). We analyzed whether SCD overexpression could modify intracellular neutral lipid deposits. Figure 6 shows a significant increase of intracellular lipid droplets in these cells, as it is can be clearly observed as larger amount of spots stained with the Oil Red reagent.

Caveolin intracellular levels and exportation

Caveolin-1 is a 22 kD protein, that, even though most of the functions are currently unclear, it has been proposed to act as Chol sensors and to regulate lipid trafficking to and from specific membrane domains, such as caveolae rich in Chol and sphingomyelin (Pol et al., 2004). It should have therefore intracellular and extracellular lipid transport-related functions. In addition, its expression has been associated with apoptosis in macrophages (Gargalovic and Dory, 2003). In order to check a probable relationship between membrane composition, lipid transport and caveolin function, we measured caveolin-1 levels in the cells and in the medium in the presence and absence of apoA-I as Chol acceptor. Figure 7a shows that intracellular levels of caveolin-1 are slightly but significantly decreased in SCD cells compared with Control cells; apoA-I has no significant effect on the levels of this protein (not shown). In order to characterize caveolin-1 exportation, and the influence that apoA-I could have in such event, we incubated cells as described above, and analyzed the extracellular medium by native gradient polyacrylamide gel electrophoresis (PAGGE), with or without incubation with apoA-I for 12 h. Interestingly, caveolin-1 was significantly more exported in SCD overexpressing cells, associated to products with molecular weights around 80 and 150kD (Figure 7b, panel i). Incubation with apoA-I did not induce strong effect on such levels. In addition, to analyze the interaction of apoA-I with caveolin, we performed a gel under the same conditions, but revealed using a polyclonal anti-apoA-I antibody; as Figure 7b, panel ii shows, most of the apoA-I remains as small, lipid-poor particles, and in a lesser extent, as big complexes, probably associated with different amounts of solubilized lipids. Nevertheless, it is clear that no apoA-I was associated with the 80 or 150 kD complexes co-migrating with caveolin.

Discussion

Mammalian cells are required to keep a dynamic arrangement of lipids and proteins as a basal mechanism to organize their structure and viability. Such events are strictly regulated by the membrane organization, which determines the intensity of multiple signaling cascades (Simons and Toomre, 2000). Our results strongly support the hypothesis that PM is clue in order to avoid citotoxic pools of Chol, thus helping cell viability. Many mechanisms could be involved in such events, and we will consider some of them here.

1) Membrane composition and fluidity

As mentioned above, in spite of the different lipid composition, PM of SCD-cell keeps the average water content (i.e fluidity) than Control cells. We considered this finding really interesting as it strongly suggests that SCD overexpression triggered compensating chemical changes to prevent alteration of the PM properties. This compensation could be explained by relative changes in Chol and SM (Figure 2).

It was recently shown that a decrease in membrane fluidity favors Chol efflux (Nandi et al., 2009). Due to the well-preserved water content that we observed for membranes of unperturbed cells (Figure 3), we conclude that membrane fluidity is important to keep cell functionality but is not probably mediating in Chol efflux.

2) Domains organization and cell interaction with different Chol acceptors

Our results show that GP decreases when Chol is removed by apoA-I from both types of cells (Figure 3d); instead, a significant increase of the GP at the PM of Control cells, and a decrease of the GP of SCD-cells membranes (Figure 3e) were observed when the Chol acceptor was MβCD. Based on our previous data using model systems (Sanchez et al., 2007a) we could suggest that Chol is solubilized from highly ordered domains from Control cells, and from disordered domains from SCD-cells. Nevertheless, due to the complexity of the membrane organization, and the dynamics of lipid rearrangement, other possibilities cannot be discarded, though they are not discussed here. Clearly, the treatment with the two Chol acceptors (MβCD and apoA-I) reveals two issues: 1) the Control and SCD-cells plasma membranes are different, but the cells *in vivo* compensate this difference in order to keep their viability, and 2) Chol efflux mediated by apoA-I and MβCD induces different membrane lipid reorganization.

It was observed that SCD-cells show a lower efficiency for Chol removal mediated by apoA-I. We have observed that this behavior is also valid when cells are loaded with external Chol (not shown). This decreased efficiency for Chol efflux cannot be explained by a special membrane composition which binds Chol with high affinity; the lipid composition found in SCD-cells -a significant lower amount of SM, together with an increase in unsaturated fatty acids- should result instead in a higher tendency of Chol to "escape" from the membrane (Lange and Steck, 2008; Simons and Vaz, 2004) and hence to be exported. The fact that Chol removal by apoA-I increases mitochondrial activity preferentially from SCD-cells suggests that the relative decrease of sphingomyelin respect to glycerophospholipids induces domain organization with Chol solublized into pools more available to acceptors as apoA-I and then favorable to be exported. In this line of thoughts, Kellner-Weibel and Rothblat postulated that apoA-I removes a cytotoxic pool of Chol which is at the plasma membrane (Kellner-Weibel et al., 1999). Our data suggest that this pool could be selectively solubilized, especially from SCD, showing higher mitochondrial activity and less LDH release (Figure 5).

3) Intracellular trafficking

In close relation with the concepts above mentioned, intracellular mobilization of Chol is strongly dependent on membrane organization. It has been shown that the highest concentration of caveolin is found in the PM, in caveolae rich in Chol and sphingolipids (Williams and Lisanti, 2004).. In addition to the membrane-bound state, this protein also has a soluble cytoplasmatic form, as well as a secreted form, both of them embedded in lipoprotein-like particles (Liu et al., 1999; Liu et al., 2002). Our results showed that SCDcells presented lesser amounts of caveolin, probably due to a higher secretion. This effect could be explained due to the lower relative amounts of SM respect to glycerophospholipids at the PM, which destabilizes caveolae and favor its exportation to the media (Figure 7). In addition, it is interesting that, even though SCD-cells show lower efficiency to export Chol (Sun et al., 2003), they are less susceptible to Chol citotoxicity (Figure 5). Our results support the fact that the lowest Chol efflux is associated with a higher cellular CE/FC ratio, and with a clear increment of intracellular lipid depots (Figure 6). The decreased levels in caveolin could, as Frank et al suggested, induce the increase observed in CE/FC ratio (Frank et al., 2006).

The characteristic of the exported caveolin is not well-known. Some cells secrete caveolin in High Density Lipoproteins (HDL) containing apoA-I, raising the possibility that caveolin-rich lipid particles in the cytoplasm are involved in the assembly of secreted lipoproteins and regulation of lipid export (Liu et al., 2002). These authors did not detect such type of vesicles in CHO cells, and our results showed that only a small amount of caveolin is secreted from Control cells either in the absence (Figure 7bi) or the presence of apoA-I (Figure 7bii). Instead, a significant amount of this protein showing a molecular weight around 80 and 150 kD is exported from SCD cells (Figure 7bi, lines 3 and 4). It does not co-migrate with apoA-I (Figure 7bii), and it is associated with fractions of density higher than 1.21 g/mL (not shown). Thus,

these exportation products do not seem to be assembled as HDL lipoproteins, but, as caveolin oligomers disassembled from the plasma membrane, due to the poor platform offered by lipids in SCD-cells (low SM and high unsaturated phospholipids).

As a conclusion, our results show that membrane composition and organization coordinate cellular pathways involved in Chol efflux and cell viability by different mechanisms. While the entire membrane fluidity is preserved, disruption of sphingomyelin-rich domains induces the solubilization of Chol into pools accessible to apoA-I and favors caveolin turn over which prone intracellular storages of non toxic cholesteryl esters. This signaling event might be complex and some other proteins (as SCP-2) are likely to participate in Chol transport and efflux. Further research will be focused in this field.

Acknowledgments

References

Bagatolli LA, Sanchez SA, Hazlett T, Gratton E. Giant vesicles, Laurdan, and two-photon fluorescence microscopy: evidence of lipid lateral separation in bilayers. Methods Enzymol 2003;360:481–500. [PubMed: 12622164]

Bligh EG, Dyer WJ. A rapid method of total lipid extraction and purification. Can J Biochem Physiol 1959;37:911–917. [PubMed: 13671378]

Bradford MM. A rapid and sensitive method for the quantitation of microgram quantities of protein utilizing the principle of protein-dye binding. Anal Biochem 1976;72:248–254. [PubMed: 942051]

Cezanne L, Navarro L, Tocanne JF. Isolation of the plasma membrane and organelles from Chinese hamster ovary cells. Biochim Biophys Acta 1992;1112:205–214. [PubMed: 1457453]

De Felice FG, Houzel JC, Garcia-Abreu J, Louzada PR Jr, Afonso RC, Meirelles MN, Lent R, Neto VM, Ferreira ST. Inhibition of Alzheimer's disease beta-amyloid aggregation, neurotoxicity, and in vivo deposition by nitrophenols: implications for Alzheimer's therapy. Faseb J 2001;15:1297–1299. [PubMed: 11344119]

Enoch HG, Catala A, Strittmatter P. Mechanism of rat liver microsomal stearyl-CoA desaturase. Studies of the substrate specificity, enzyme-substrate interactions, and the function of lipid. J Biol Chem 1976;251:5095–5103. [PubMed: 8453]

Fielding PE, Nagao K, Hakamata H, Chimini G, Fielding CJ. A two-step mechanism for free cholesterol and phospholipid efflux from human vascular cells to apolipoprotein A-1. Biochemistry 2000;39:14113–14120. [PubMed: 11087359]

Folch J, Lees M, Sloane Stanley GH. A simple method for the isolation and purification of total lipides from animal tissues. J Biol Chem 1957;226:497–509. [PubMed: 13428781]

Frank PG, Cheung MW, Pavlides S, Llaverias G, Park DS, Lisanti MP. Caveolin-1 and regulation of cellular cholesterol homeostasis. Am J Physiol Heart Circ Physiol 2006;291:H677–H686. [PubMed: 16603689]

Gargalovic P, Dory L. Cellular apoptosis is associated with increased caveolin-1 expression in macrophages. J Lipid Res 2003;44:1622–1632. [PubMed: 12777465]

Gaus K, Gratton E, Kable EP, Jones AS, Gelissen I, Kritharides L, Jessup W. Visualizing lipid structure and raft domains in living cells with two photon microscopy. Proc Natl Acad Sci U S A 2003;100:15554–15559. [PubMed: 14673117]

Gonzalez MC, Toledo JD, Tricerri MA, Garda HA. The central type Y amphipathic alpha-helices of apolipoprotein AI are involved in the mobilization of intracellular cholesterol depots. Arch Biochem Biophys 2008;473:34–41. [PubMed: 18316036]

Harris FM, Best KB, Bell JD. Use of laurdan fluorescence intensity and polarization to distinguish between changes in membrane fluidity and phospholipid order. Biochim Biophys Acta 2002;1565:123–128. [PubMed: 12225860]

Heiner AL, Gibbons E, Fairbourn JL, Gonzalez LJ, McLemore CO, Brueseke TJ, Judd AM, Bell JD. Effects of cholesterol on physical properties of human erythrocyte membranes: impact on susceptibility to hydrolysis by secretory phospholipase A2. Biophys J 2008;94:3084–3093. [PubMed: 18192373]

Jacobson K, Mouritsen OG, Anderson RG. Lipid rafts: at a crossroad between cell biology and physics. Nature Cell Biology 2007;9:7–14.

Kellner-Weibel G, Geng YJ, Rothblat GH. Cytotoxic cholesterol is generated by the hydrolysis of cytoplasmic cholesteryl ester and transported to the plasma membrane. Atherosclerosis 1999;146:309–319. [PubMed: 10532697]

Lange Y, Steck TL. Cholesterol homeostasis and the escape tendency (activity) of plasma membrane cholesterol. Prog Lipid Res 2008;47:319–332. [PubMed: 18423408]

Liu P, Li WP, Machleidt T, Anderson RG. Identification of caveolin-1 in lipoprotein particles secreted by exocrine cells. Nat Cell Biol 1999;1:369–375. [PubMed: 10559965]

Liu P, Rudick M, Anderson RG. Multiple functions of caveolin-1. J Biol Chem 2002;277:41295–41298. [PubMed: 12189159]

Lowry OH, Rosebrough NJ, Farr AL, Randall RJ. Protein measurement with the Folin phenol reagent. J Biol Chem 1951;193:265–275. [PubMed: 14907713]

Mander EL, Dean RT, Stanley KK, Jessup W. Apolipoprotein B of oxidized LDL accumulates in the lysosomes of macrophages. Biochim Biophys Acta 1994;1212:80–92. [PubMed: 8155730]

Melchert RB, Liu H, Granberry MC, Kennedy RH. Lovastatin inhibits phenylephrine-induced ERK activation and growth of cardiac. Cardiovasc Toxicol 2001;1:237–252. [PubMed: 12213976]

Mendez AJ, Lin G, Wade DP, Lawn RM, Oram JF. Membrane lipid domains distinct from cholesterol/sphingomyelin-rich rafts are involved in the ABCA1-mediated lipid secretory pathway. J Biol Chem 2001;276:3158–3166. [PubMed: 11073951]

Montes LR, Alonso A, Goni FM, Bagatolli LA. Giant unilamellar vesicles electroformed from native membranes and organic lipid mixtures under physiological conditions. Biophys J 2007;93:3548–3554. [PubMed: 17704162]

Nandi S, Ma L, Denis M, Karwatsky J, Li Z, Jiang XC, Zha X. ABCA1-mediated cholesterol efflux generates microparticles in addition to HDL through processes governed by membrane rigidity. J Lipid Res 2009;50:456–466. [PubMed: 18941142]

Oram JF. ATP-binding cassette transporter A1 and cholesterol trafficking. Curr Opin Lipidol 2002;13:373–381. [PubMed: 12151852]

Oram JF, Heinecke JW. ATP-binding cassette transporter A1: a cell cholesterol exporter that protects against cardiovascular disease. Physiological Reviews 2005;85:1343–1372. [PubMed: 16183915]

Parasassi T, Gratton E. Membrane lipid domains and dynamics as detected by Laurdan fluorescence. J. Fluorescence 1995;8:365–373.

Parasassi T, Gratton E, Yu WM, Wilson P, Levi M. Two-photon fluorescence microscopy of laurdan generalized polarization domains in model and natural membranes. Biophys J 1997;72:2413–2429. [PubMed: 9168019]

Peter A, Weigert C, Staiger H, Rittig K, Cegan A, Lutz P, Machicao F, Haring HU, Schleicher E. Induction of stearoyl-CoA desaturase protects human arterial endothelial cells against lipotoxicity. Am J Physiol Endocrinol Metab 2008;295:E339–E349. [PubMed: 18523127]

Pol A, Martin S, Fernandez MA, Ferguson C, Carozzi A, Luetterforst R, Enrich C, Parton RG. Dynamic and regulated association of caveolin with lipid bodies: modulation of lipid body motility and function by a dominant negative mutant. Mol Biol Cell 2004;15:99–110. [PubMed: 14528016]

Prinz WA. Non-vesicular sterol transport in cells. Progress in Lipid Research 2007;46:297–314. [PubMed: 17709145]

Sambrook, J.; Fritsch, EF.; Maniatis, T. N.Y. Cold Spring Harbor; 1989. Molecular cloning: a laboratory manual; p. 938-957.

Sanchez SA, Bagatolli LA, Gratton E, Hazlett TL. A two-photon view of an enzyme at work: Crotalus atrox venom PLA2 interaction with single-lipid and mixed-lipid giant unilamellar vesicles. Biophys J 2002;82:2232–2243. [PubMed: 11916878]

Sanchez SA, Tricerri MA, Gratton E. Interaction of high density lipoprotein particles with membranes containing cholesterol. J Lipid Res 2007a;48:1689–1700. [PubMed: 17485728]

Sanchez, SA.; Tricerri, MA.; Gunther, G.; Gratton, E. Laurdan Generalized Polarization: from cuvette to microscope. Modern Research and Educational Topics in Microscopy. Applications in Physical/ Chemical Sciences. In: V.a.D., AM., editor. Modern Research and Educational Topics in Microscopy. Applications in Physical/Chemical Sciences. 2007b. p. 1007-1014.

Schroeder F, Atshaves BP, McIntosh AL, Gallegos AM, Storey SM, Parr RD, Jefferson JR, Ball JM, Kier AB. Sterol carrier protein-2: new roles in regulating lipid rafts and signaling. Biochim Biophys Acta 2007;1771:700–718. [PubMed: 17543577]

Schroeder F, Gallegos AM, Atshaves BP, Storey SM, McIntosh AL, Petrescu AD, Huang H, Starodub O, Chao H, Yang H, Frolov A, Kier AB. Recent advances in membrane microdomains: rafts, caveolae, and intracellular cholesterol trafficking. Exp Biol Med (Maywood) 2001;226:873–890. [PubMed: 11682693]

Simons K, Toomre D. Lipid rafts and signal transduction. Nat Rev Mol Cell Biol 2000;1:31–39. [PubMed: 11413487]

Simons K, Vaz WL. Model systems, lipid rafts, and cell membranes. Annu Rev Biophys Biomol Struct 2004;33:269–295. [PubMed: 15139814]

Smith JD, Le Goff W, Settle M, Brubaker G, Waelde C, Horwitz A, Oda MN. ABCA1 mediates concurrent cholesterol and phospholipid efflux to apolipoprotein A-I. J Lipid Res 2004;45:635–644. [PubMed: 14703508]

Smith SK, Farnbach AR, Harris FM, Hawes AC, Jackson LR, Judd AM, Vest RS, Sanchez S, Bell JD. Mechanisms by which intracellular calcium induces susceptibility to secretory phospholipase A2 in human erythrocytes. J Biol Chem 2001;276:22732–22741. [PubMed: 11294854]

So PTC, French T, Yu WM, Berland KM, Dong CY, Gratton E. Time resolved fluorescence microscopy using two photon excitation. Bioimaging 1995;3:49–63.

Storey SM, Gallegos AM, Atshaves BP, McIntosh AL, Martin GG, Parr RD, Landrock KK, Kier AB, Ball JM, Schroeder F. Selective cholesterol dynamics between lipoproteins and caveolae/lipid rafts. Biochemistry 2007;46:13891–13906. [PubMed: 17990854]

Sun Y, Hao M, Luo Y, Liang CP, Silver DL, Cheng C, Maxfield FR, Tall AR. Stearoyl-CoA desaturase inhibits ATP-binding cassette transporter A1-mediated cholesterol efflux and modulates membrane domain structure. J Biol Chem 2003;278:5813–5820. [PubMed: 12482877]

Sviridov D, Fidge N, Beaumier-Gallon G, Fielding C. Apolipoprotein A–I stimulates the transport of intracellular cholesterol to cell-surface cholesterol-rich domains (caveolae). Biochem J 2001;358:79–86. [PubMed: 11485554]

Tricerri A, Corsico B, Toledo JD, Garda HA, Brenner RR. Conformation of apolipoprotein AI in reconstituted lipoprotein particles and particle-membrane interaction: effect of cholesterol. Biochim Biophys Acta 1998;1391:67–78. [PubMed: 9518555]

Tricerri MA, Toledo JD, Sanchez SA, Hazlett TL, Gratton E, Jonas A, Garda HA. Visualization and analysis of apolipoprotein A–I interaction with binary phospholipid bilayers. J Lipid Res 2005;46:669–678. [PubMed: 15654128]

Weber G, Farris FJ. Synthesis and spectral properties of a hydrophobic fluorescent probe: 6-propionyl-2-(dimethylamino)naphthalene. Biochemistry 1979;18:3075–3078. [PubMed: 465454]

Williams TM, Lisanti MP. The caveolin proteins. Genome Biol 2004;5:214. [PubMed: 15003112]

Yamauchi Y, Chang CC, Hayashi M, Abe-Dohmae S, Reid PC, Chang TY, Yokoyama S. Intracellular cholesterol mobilization involved in the ABCA1/apolipoprotein-mediated assembly of high density lipoprotein in fibroblasts. J Lipid Res 2004;45:1943–1951. [PubMed: 15292375]

Yancey PG, Bortnick AE, Kellner-Weibel G, de la Llera-Moya M, Phillips MC, Rothblat GH. Importance of different pathways of cellular cholesterol efflux. Arterioscler Thromb Vasc Biol 2003;23:712–719. [PubMed: 12615688]
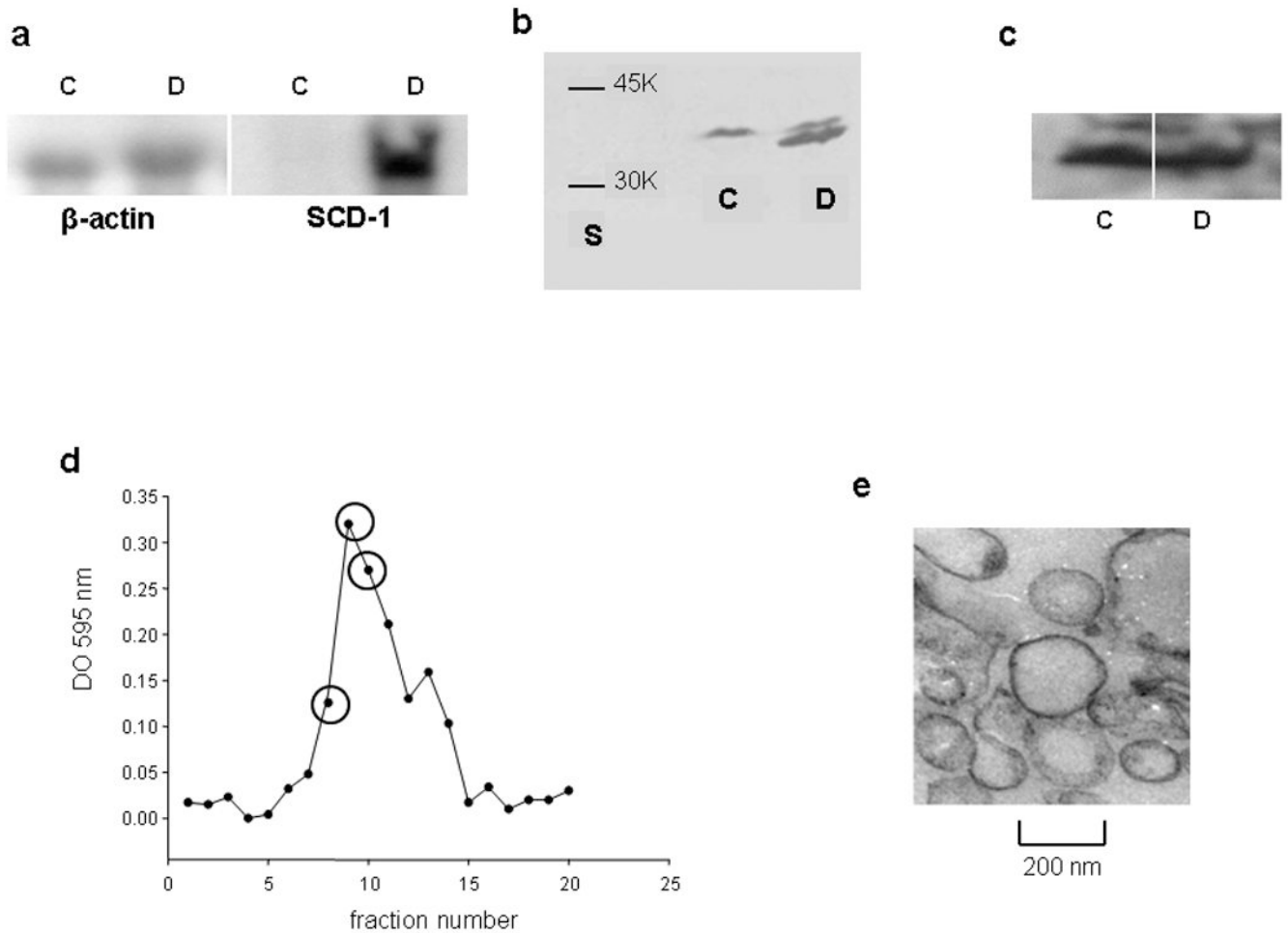
Figure 1. SCD-cell line characterization

a) Overexpression of SCD determined by Northern blot: Twenty µg of total RNA were loaded in each well and SCD overexpression (symbol D) respect to the control (symbol C) was determined by comparison with β-actin as described in Methods. b) Protein levels of SCD detected by western blot. One hundred fifty µg of total protein of the membrane pellet was resuspended in sample buffer containing SDS and β mercaptoethanol, boiled and resolved in a homogeneous 12 % gel with 10 % SDS. Lane S corresponds to molecular weight markers. c) ABCA1 protein levels were detected in a similar manner. Samples without boiling treatment were separated in a 4–15% gradient gel containing SDS. d) Typical elution profile obtained for membrane purification. Each 200 µL from the top of the Nicodenz-Ficoll gradient were tested for protein content (Bradford, 1976). Fractions labeled with an empty circle were pooled and further analyzed to confirm the presence and purity of plasma membrane. e) Transmission electron micrograph of the isolated plasma membrane fraction. Magnification 20 K.
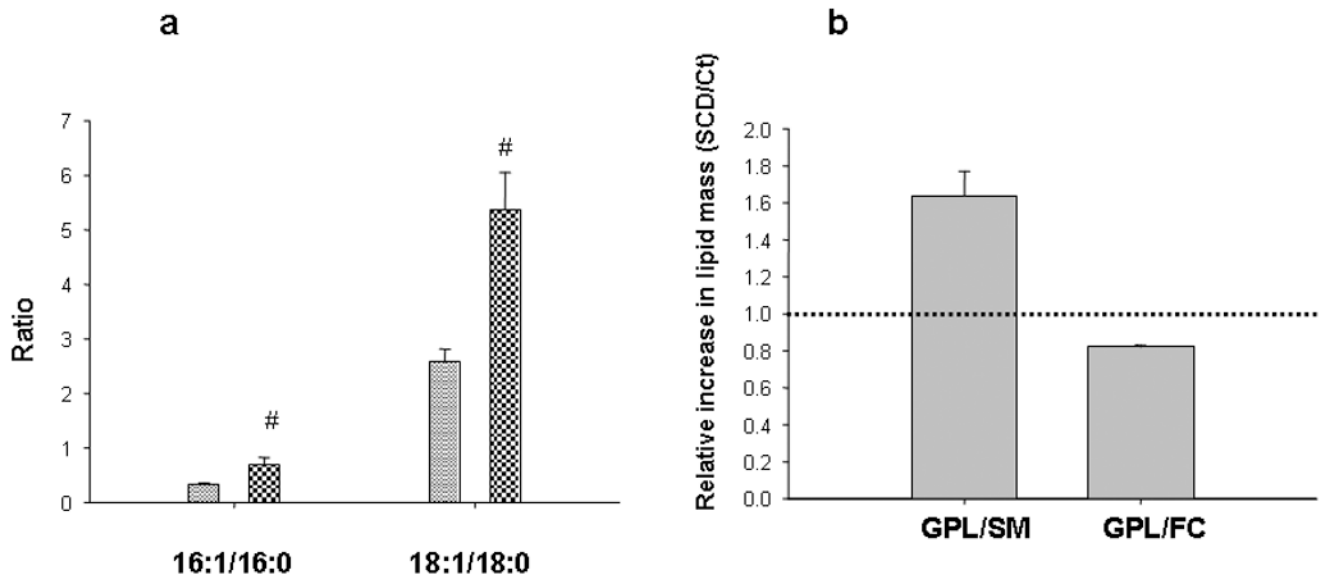
Figure 2. Lipid composition of the SCD-cells plasma membrane respect to Control Cells
a) Total lipids from the plasma membrane fraction were extracted and fatty acids composition determined by GLC, after trans esterification with B3F. Bars show 16:1/16:0 and 18:1/18:0 ratios of SCD-cells (checkered bars) respect to Control (dashed bars) Symbol # means significant difference as compared with Control cells ($P<0.05$). b) Plasma total lipids were separated by TLC and composition quantified by scanning of different lipid areas after calcination. Figure shows the relative ratios of glycerophospholipids (GPL) to sphingomyelin (SM) and to free cholesterol (FC) in SCD cells respect to Control (Ct). Dot line shows ratio=1, to better visualize the relative changes induced by the overexpression of SCD.
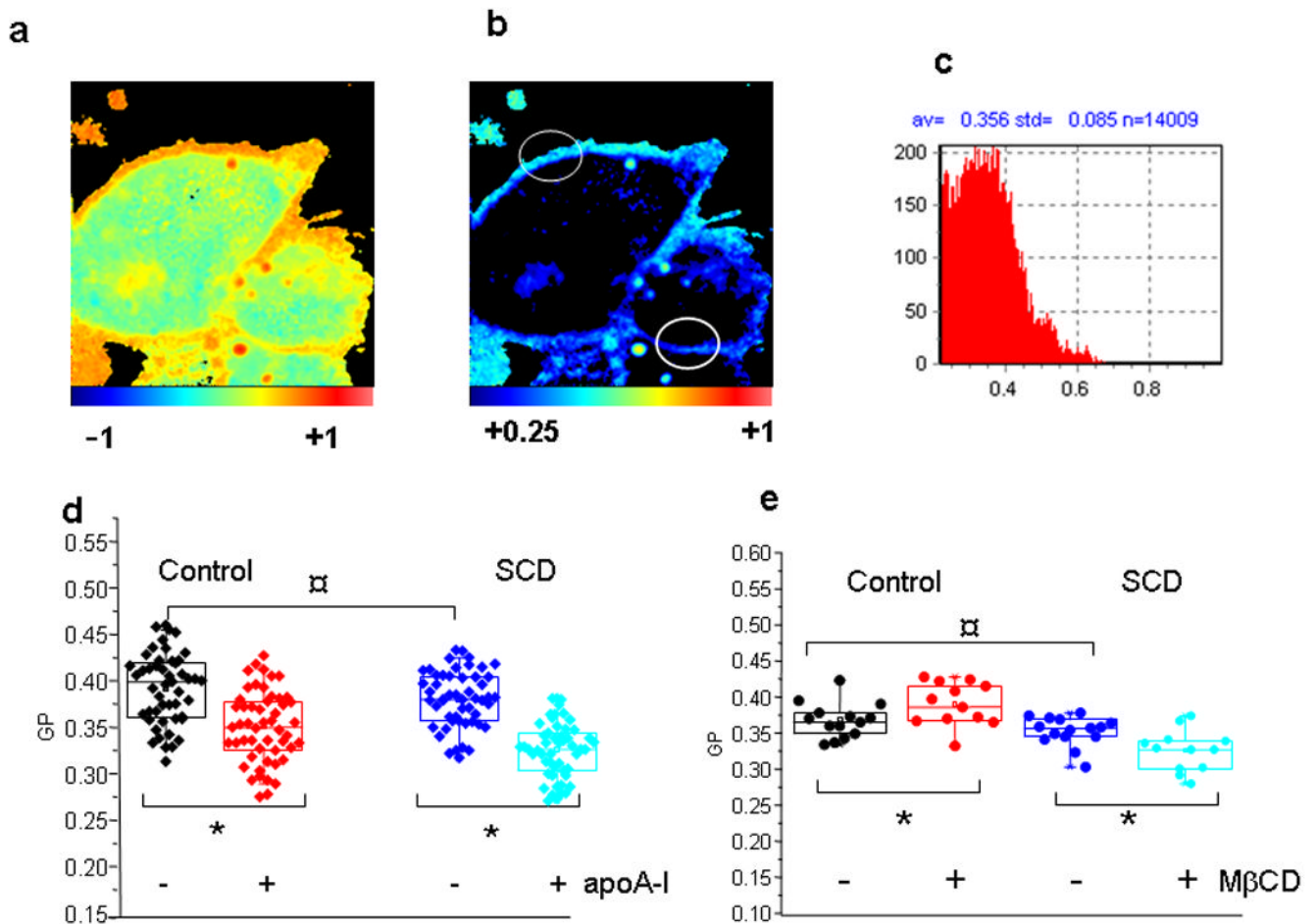
**Figure 3. Laurdan GP two-photon fluorescence microscopy of CHO cells**
a) Cells were grown as described previously, and stained with Laurdan for 15 minutes. Laurdan GP images were taken as described, focusing at the middle plane of the cell. b) The same figure than a), but with a modification in the color scale, to eliminate the interference of pixels with lower GP values (from the Laurdan solubilized into the cytoplasm) (see scale at the bottom of the figure). Empty white circles symbolize the selected areas for GP analysis. Each histogram of GP values of these areas (represented in c), is used to calculate the experimental data shown in panels d and e. e) Experimental values of GP at the plasma membrane in unperturbed Control (black) and SCD-cells (blue symbols). Box-Charts show minimum, 25th percentile, median and 75th percentile values. GP was also measured in the same way after overnight incubation of Control (red) and SCD-cells (cyan symbols) with 20 µg/mL apoA-I. No difference was detected among samples without addition of apoA-I (¤ symbol, with $P<0.05$). Instead, GP decreased significantly for both types of cells after the addition of apoA-I (* symbols, $P<0.05$). e) Cells (Control and overexpressing SCD), were incubated in the absence or in the presence of 10 mM MβCD for 30 min. Experimental data are analyzed as in Figure d. As in d, statistically non difference is shown with ¤, while * represents a significant increase or decrease of membrane GP after treatment with MβCD of Control or SCDcells, respectively ($P<0.05$).
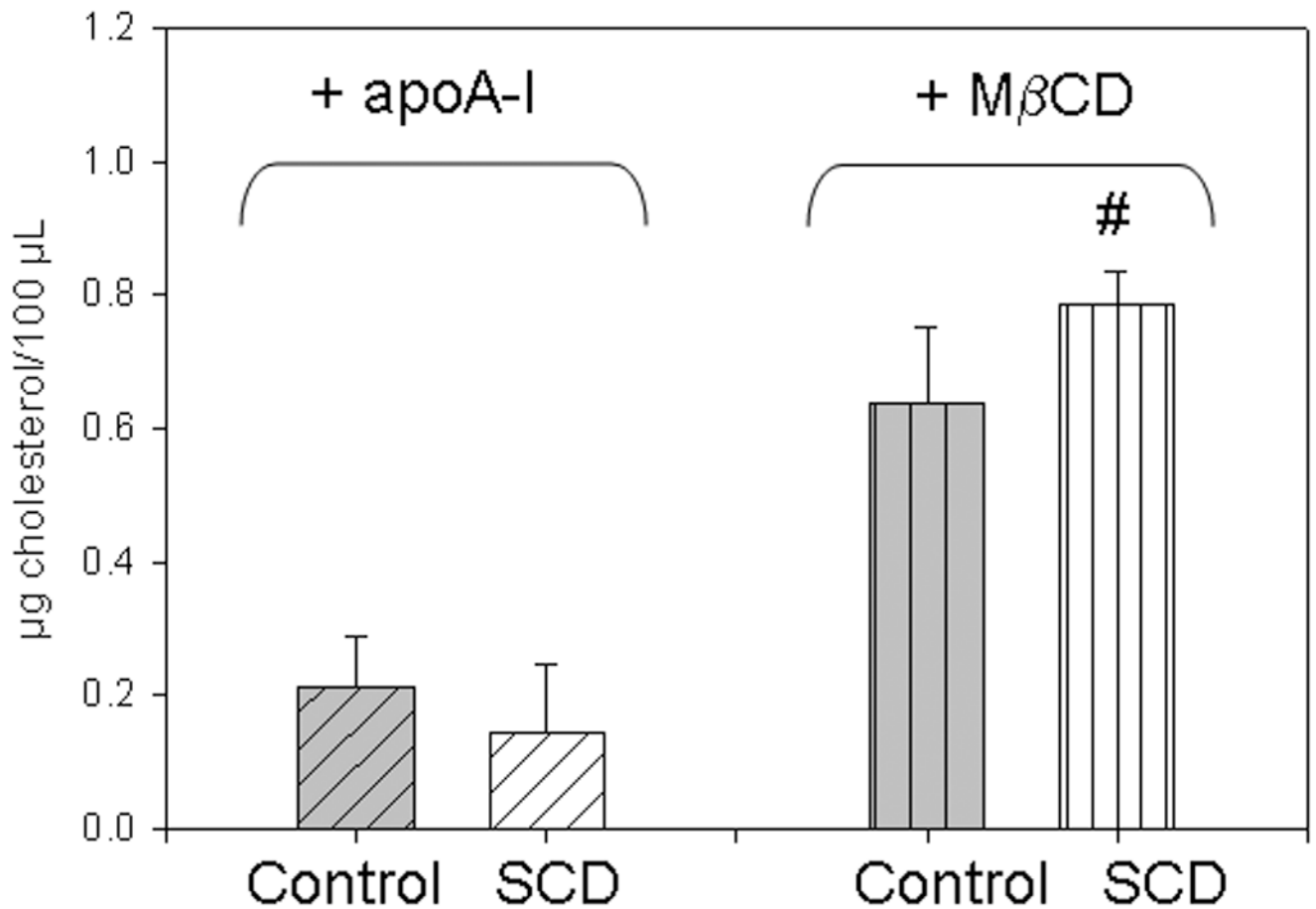
**Figure 4. Cholesterol removal to different acceptors**
Cells were in a 96 well-plate and incubated as described above, overnight in the presence of
20 µg/mL apoA-I (diagonally-lined bars), or by 30 min with 10 mM MβCD (vertically-lined
bars). Cholesterol in the media at the end of the treatments was analyzed as described in
Methods. Symbol * indicates statistic increase of Chol removal by SCDcells (white filled), as
respect to Control cells (gray filled bars) ($P < 0.05$)
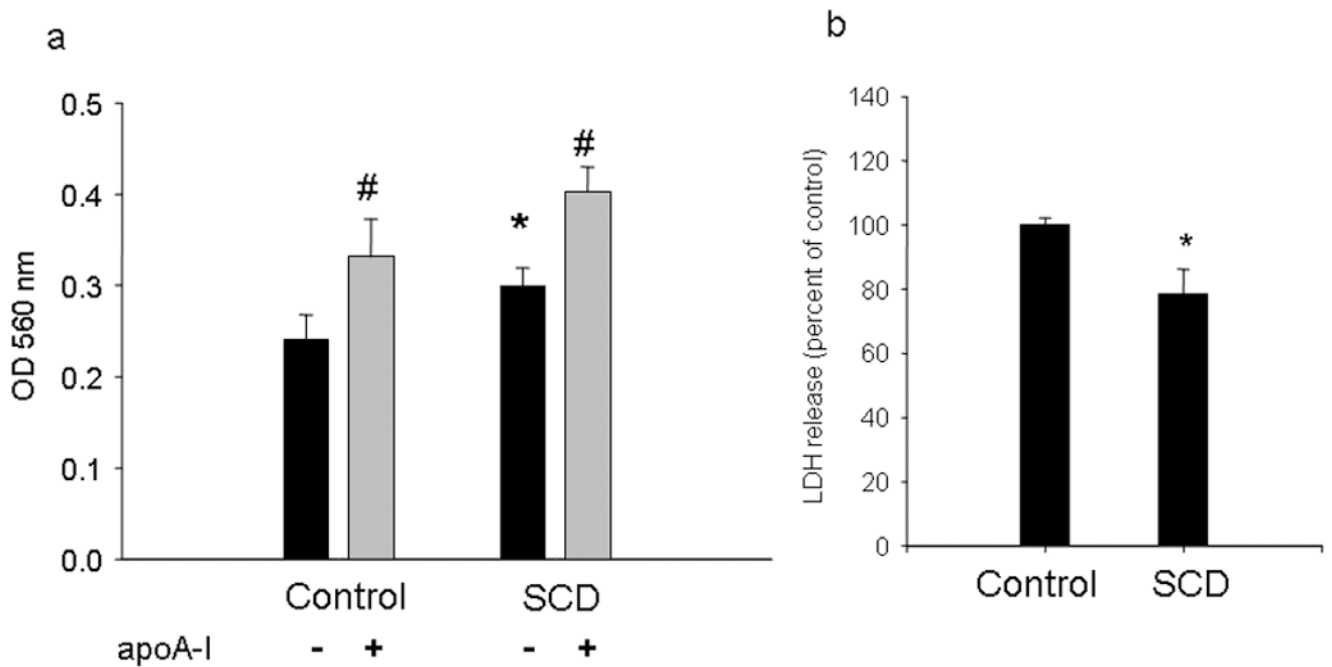
Figure 5. Cellular viability
a) Mitochondrial metabolism assay: Cells were grown in a 96-well microplate, and MTT reduction was evaluated with or without overnight incubation with 20 µg/mL apoA-I. The formation of formazan was quantified by absorbance at 560 nm (*$P < 0.05$ compared to Control, untreated cultures; # indicates $P < 0.05$ compared to the same type of cells incubated in the absence of apoA-I). Results are the means of 5 experimental points. b) Lactate dehydrogenase (LDH) release into the medium. Cells were grown as explained in Methods, and LDH in the medium was determined by kinetics of disappearance of NADH at 340 nm. Results are the means of triplicate samples.(*$P < 0.05$ compared to Control, untreated cultures).
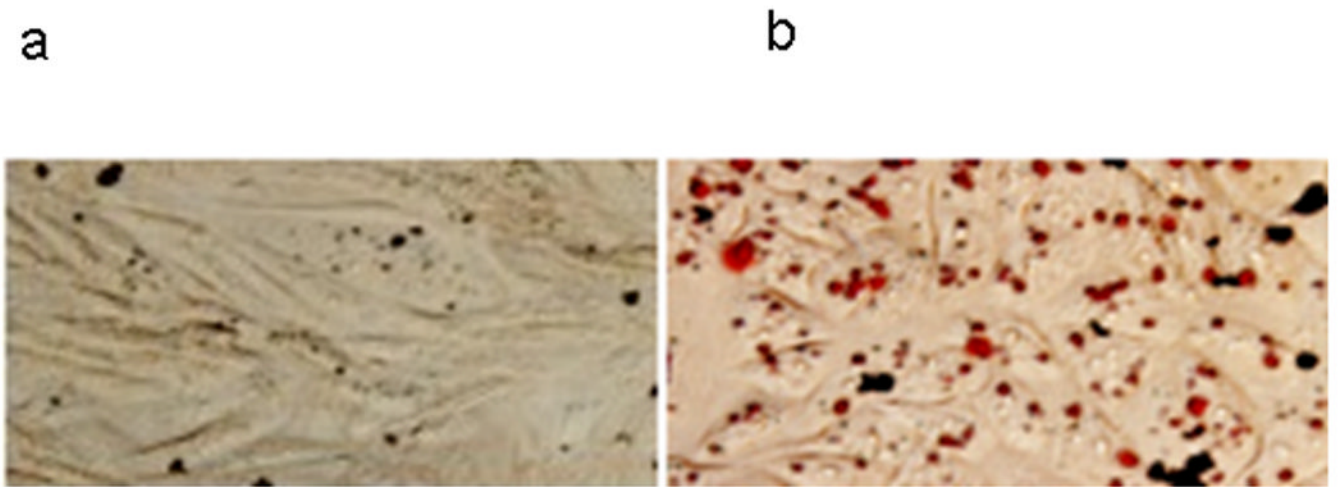
Figure 6. Observation of intracellular lipid droplets
Cells were fixed and stained with Oil-O Red as explained in the Methods section. Observation was made in an Olympus BX51 microscope. Intracellular red spots correspond to lipid accumulations. a) Control cells b) SCD-cells
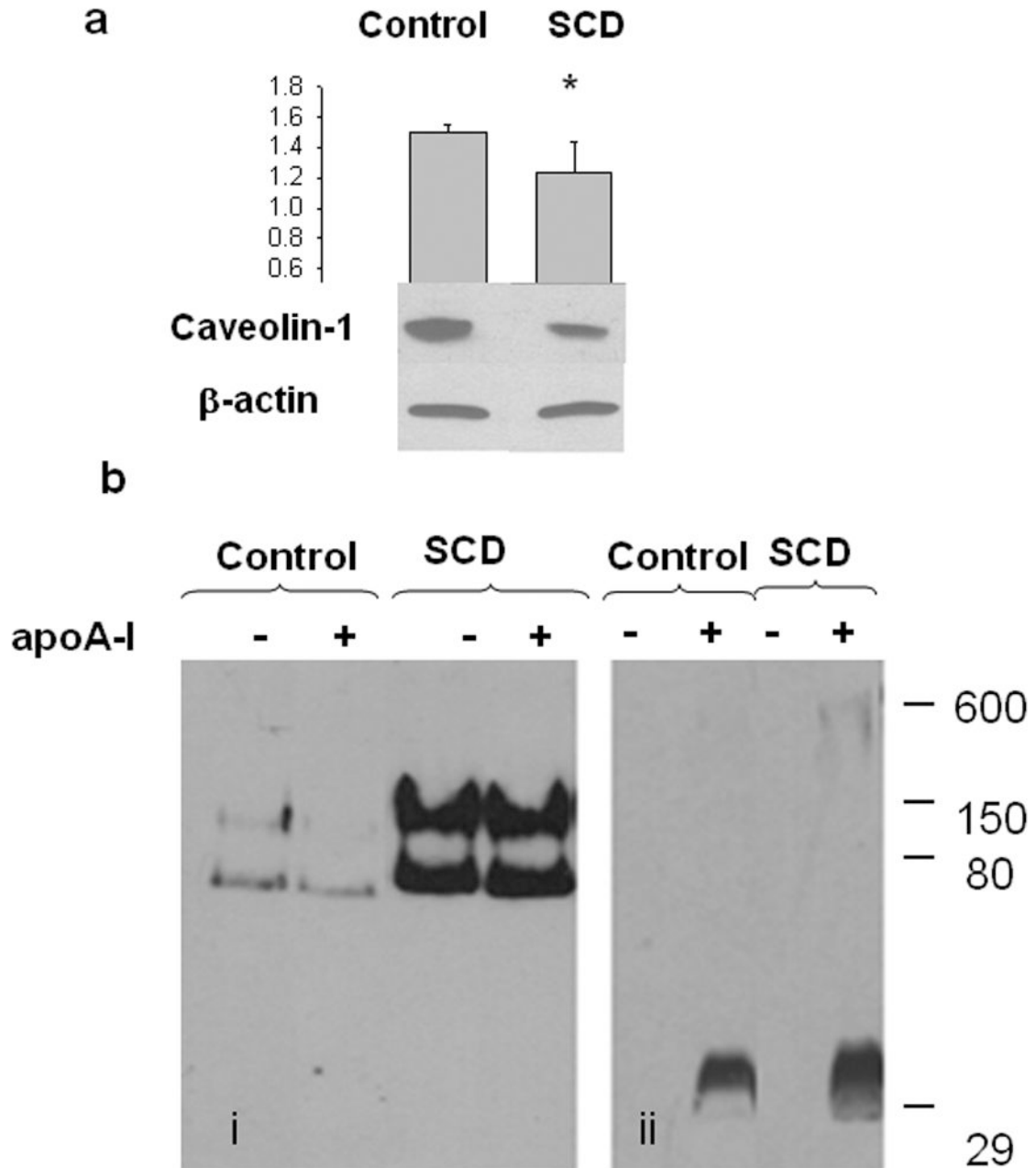
Figure 7. Intracellular and exportation levels of caveolin-1

a) Control and SCD-cells were grown and incubated as previously described. Following culture cells were scrapped, lysed and homogenized. The same amount of protein from the different treatments was loaded on a 12 % PAGE with 10% SDS, western blot developed against a-caveolin and following stripping developed against β actin. Bands of four different samples of Control or SCD-cells were scanned and the relative intensity of each band quantified by the Image Quant software. The ratio caveolin/actin averaged and shown in the top panel.(*$P < 0.05$ compared to Control, untreated cultures).

b) Control and SCD-cells were grown and incubated with apoA-I as previously described. After 12 h incubation with DMEM or apoA-I, media was collected, centrifuged for 15 minutes at

5.000 rpm, and concentrated; the same amount of total protein of the different treatments was loaded on a native 4–25% polyacrylamide gradient electrophoresis gel (bi) and revealed by using polyclonal caveolin-1 antibody. bii) An equivalent gel was loaded and run exactly under the same conditions, but revealed against polyclonal a-apoA-I. Numbers on the right side of the Figure correspond to molecular weight standards.